JETIR.ORG ISSN: 2349-5162 | ESTD Year : 2014 | Monthly Issue
JOURNAL OF EMERGING TECHNOLOGIES AND INNOVATIVE RESEARCH (JETIR)
An International Scholarly Open Access, Peer-reviewed, Refereed Journal

Literature Survey of recursive static state estimation algorithm

Tamal Ghosh,
Student (M-tech),
Department of Electrical Engineering,
JIS College of Engineering, Kalyani, India.

Dr. Alok Kumar Shrivastav,
Head of the Department,
Department of Electrical Engineering,
JIS College of Engineering, Kalyani, India.

Abstract:

Prior to state estimation, an observability analysis must be performed to make sure the measurements (e.g. power injection and flow measurements) received can support the normal functioning of the state estimator. If the measurements cannot provide full observability of the network, the observability analysis function identifies the observable islands where state estimation can still be performed within the observable islands. In this thesis it is shown that the existing method may not correctly identify the observable islands in the so called pathological cases; the thesis proposes a new method for observability analysis that overcomes this problem. Furthermore the execution time of the proposed method is shorter than existing methods. To support the deployment of the SMT in state estimation, the thesis also proposes a new method for including the synchronised measurements in the observability analysis function.

Key Word : Measurements, Power system, State estimation, Recursive estimation, Weighted least square, observability, Jacobian.

Introduction:

State estimation is responsible for constantly monitoring the power system to help guarantee that it operates in a normal and secure state. It uses a redundant set of measurements to produce the optimal estimate of the system's current operating state. The state estimator plays a key role in the Energy Management Systems (EMS), which are equipped with various other applications. Figure 2-1 shows an example of how the state estimator functions with various applications involved in the online static security assessment procedure. As detailed in the introduction, the function of the state estimator is supported by functions that include topology processor, observability analysis and bad data detection. Based on the estimate of the voltage angle and magnitudes of all the buses in the network, one of the three states is determined: emergency, restorative and normal. If the system is determined to be operating in emergency state or restorative state, the corresponding

emergency control or restorative control will be activated. If the system is found to be in a normal state, it is assessed using a contingency analysis application to further check the security of the system. In the case of insecurity state, while the system is at risk of some contingencies, the preventive actions need to be planned after running the security constrained optimal power flow.

Although the DSEs have shown their advantages with the advent of SMT, the static state estimator (SSE) has formed the heart of nearly all modern network control systems since its establishment in the early 1970s. The SSE obtains the voltage phasors at a given point in time using the Weighted Least Square (WLS) method. The WLS method is derived under the Gaussian error assumption and the maximum likelihood estimation (MLE) theory. It guarantees that the estimate is the most likely state of the system based on the measurements received. Although it is suggested that some robust estimators, such as weighted least absolute value (WLAV) estimators and M-estimators, are less vulnerable to outliers (the measurements whose errors have large influence on the estimate of states) than the WLS method, they have not been adopted by the control centres because of their heavy computational burden.

In the following sections, the algorithm of the WLS method for static state estimation, and the existing methods for observability analysis and bad data detection are presented. In the later chapters, new methods are proposed based on the basic theory presented here.

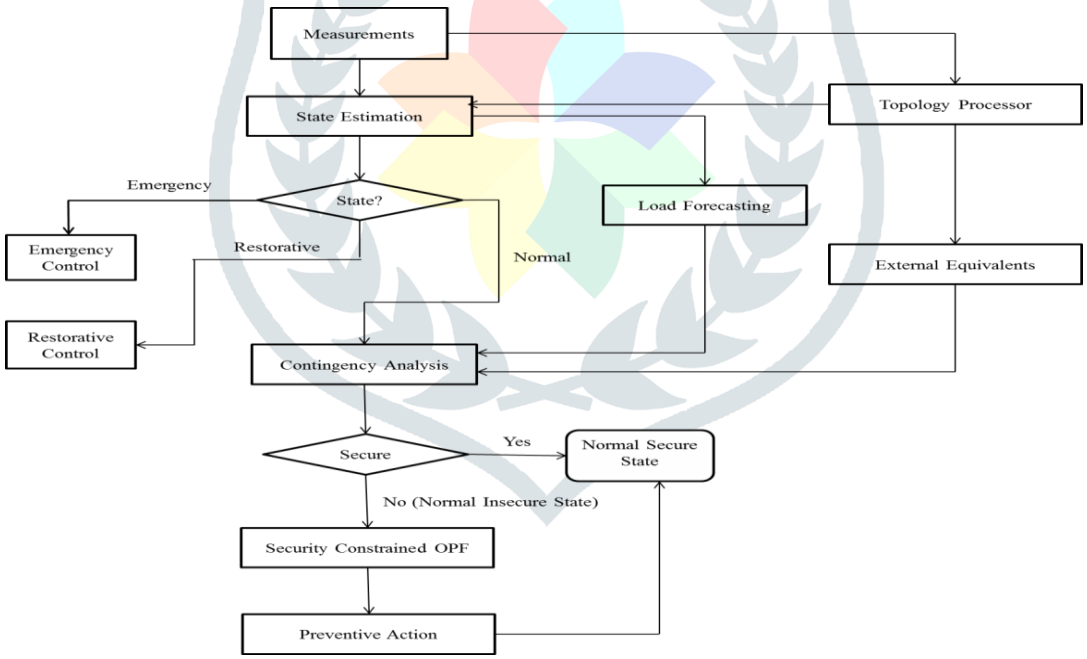

Figure 2-1: Online Static Security Assessment: Functional Diagram

List of Static State Estimation Methods:-

2. Weighted Least Square Estimator

In this subsection, a general introduction about stochastic process and random variables and detailed discussion about the weighted least square (WLS) state estimator, including the measurement functions, the WLS objective

function and its optimal solution, the measurement Jacobian matrix and the WLS state estimation algorithm, are presented.

2.1.1 Stochastic Process and Random Variables

In probability theory and related fields, a stochastic or random process is a mathematical object usually defined as a collection of random variables [94], and a random variable is defined as a variable whose possible values are numerical outcomes of a random phenomenon [95]. In power systems, the measurements received from the measurement devices installed across the network are affected by a series of random errors including device measurement errors, telecommunication errors, skew errors, loss of data. Thus, the process of measurement collection, transmission and reception is a stochastic process, and the measurements are random variables, which are commonly accepted in literature to follow the Gaussian distribution. The probability density function (p.d.f.) of the standard Gaussian distributed variable is illustrated in Figure 2-2.

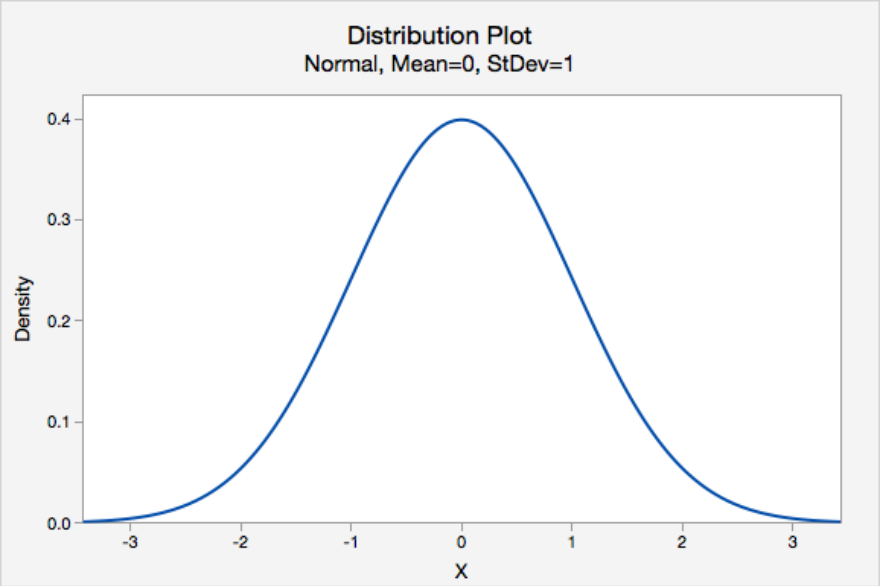

Figure 2-2: Probability Density Function of the Standard Gaussian Distribution

Since the measurements contain a certain amount of errors, a redundant set of measurements are used to monitor the states of the system. For example, the air temperature in the room is 27 °C, and is simultaneously monitored by five thermometers. The readings of the five thermometers are 27.3 °C, 26.5 °C, 27.2 °C, 26.9 °C and 27.2 °C, respectively. Since all of the five thermometers are affected by random errors, the most likely temperature is the average of the five numbers, 27.02 °C, which is very close to the true temperature in the room. Here, the room is the system, the room temperature is the state of system, the average value of the readings of the five thermometers is the estimate of states, and the average function is the estimator. In general, an estimator can be defined as the function or application that provide the most likely estimate of the states based on observations / measurements that are affected by random errors. There are various types of estimators created for different purposes, such as weighted least square (WLS) estimator [1], least absolute value (LAV) estimator [1], M-estimator [1], Kalman filters [164]-[167] and so on. In static state estimation for power systems, the most widely used estimator is the WLS estimator. In the following subsections, a detailed discussion of the WLS estimator will be given, as well as the measurement functions (Section 2.1.2), the

objective function and the optimal solution (Section 2.1.3), the expressions of the elements of its measurement Jacobian matrix (Section 2.1.4), and the algorithm of the WLS estimator (Section 2.1.5).

2.1.2 The Measurement Functions

A generalized formulation of the static state estimator using the WLS method utilizes five different types of conventional measurements for estimating the state of the system. The structure of the measurement vector **Z** is given below:

$$Z = \begin{bmatrix} P_{inj} \\ Q_{inj} \\ P_{flow} \\ Q_{flow} \\ V_{mag} \end{bmatrix} \tag{2.1}$$

where P_{inj}, Q_{inj}, P_{flow} & Q_{flow} are the vectors of active and reactive injection measurements and flow measurements, and V is the vector of voltage magnitude measurements. The conventional measurements are related to the states using a set of nonlinear functions as given in (2.2):

$$Z = h(x) + e \tag{2.2}$$

where x is the state vector that consists of voltage angles and magnitudes of all buses in the network, h is the vector of nonlinear functions relating the measurements and the states, and e is the vector of Gaussian errors. Note that since the conventional measurements are not synchronised like the PMU measurements, the slack bus is set usually as the reference bus. The angle of the reference bus is set at 0, and it is excluded from the state vector. Assuming the network parameters are known, the measurement equations for the five types of conventional measurement are based on the network structure in Figure 2-3 and are expressed as follows:

- Real and reactive power injection measurements

$$P_i = V_i \sum_{j=1}^{N} V_j (G_{ij} \cos\theta_{ij} + B_{ij} \sin\theta_{ij}) \tag{2.3}$$

$$Q_i = V_i \sum_{j=1}^{N} V_j (G_{ij} \sin\theta_{ij} - B_{ij} \cos\theta_{ij}) \tag{2.4}$$

- Real and reactive power flow measurements

$$P_{ij} = \frac{V_i^2}{a_{ij}^2}(g_{si} + g_{ij}) - \frac{V_i V_j}{a_{ij}}(g_{ij}\cos\theta_{ij} + b_{ij}\sin\theta_{ij}) \quad (2.5)$$

$$Q_{ij} = -\frac{V_i^2}{a_{ij}^2}(b_{si} + b_{ij}) - \frac{V_i V_j}{a_{ij}}(g_{ij}\sin\theta_{ij} - b_{ij}\cos\theta_{ij}) \quad (2.6)$$

$$P_{ji} = V_j^2(g_{sj} + g_{ij}) - \frac{V_j V_i}{a_{ij}}(g_{ij}\cos\theta_{ji} + b_{ij}\sin\theta_{ji}) \quad (2.7)$$

$$Q_{ji} = -V_j^2(b_{sj} + b_{ij}) - \frac{V_j V_i}{a_{ij}}(g_{ij}\sin\theta_{ji} - b_{ij}\cos\theta_{ji}) \quad (2.8)$$

- Voltage magnitude measurements

$$V_i = V_i \quad (2.9)$$

where G_{ij} and B_{ij} are the real and imaginary parts of the ijth element of the network admittance matrix, respectively, g_{ij} and b_{ij} are the conductance and susceptance of the transmission line, respectively, g_{si} and b_{si} are the shunt conductance and shunt susceptance of the shunt branch, respectively, and a_{ij} is the tap ratio of the transformer connecting Bus i and Bus j.

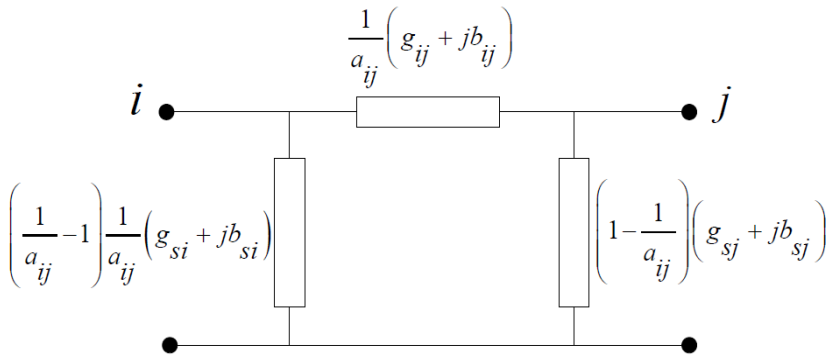

Figure 2-3: Transmission Line Represented in Pi Equivalent Model

2.1.3 The WLS Objective Function and Its Optimal Solution

According to the MLE theory, the optimal estimate of the state from the measurement equation (2.2) is achieved when the following WLS objective function is minimised:

$$J(\mathbf{x}) = \left[\mathbf{z} - \mathbf{h}(\mathbf{x})\right]^T \cdot \mathbf{R}^{-1} \cdot \left[\mathbf{z} - \mathbf{h}(\mathbf{x})\right] \quad (2.10)$$

Where **R** is the covariance matrix of the error vector, **e**. The minimum of the objective function is found when its first derivative is zero:

$$\frac{\partial J^T(\mathbf{x})}{\partial \mathbf{x}} = -2\mathbf{H}^T\mathbf{R}^{-1}\cdot\left[\mathbf{z}-\mathbf{h}(\mathbf{x})\right] = \mathbf{0}$$
$$\Rightarrow \mathbf{m}(\mathbf{x}) = \mathbf{H}^T\mathbf{R}^{-1}\left[\mathbf{z}-\mathbf{h}(\mathbf{x})\right] = \mathbf{0} \quad (2.11)$$

Where **H** is the Jacobian matrix of the measurement to state function, **h**. Since the derived objective function, **m**(**x**), is still nonlinear, it has to be iteratively solved using the Newton- Raphson method. The iteration steps are derived as given in (2.12) and (2.13).

$$\mathbf{M} = \frac{\partial \mathbf{m}^T(\mathbf{x})}{\partial \mathbf{x}} = -\mathbf{H}^T\mathbf{R}^{-1}\mathbf{H} \quad (2.12)$$

$$\Delta\mathbf{x}^k = -\mathbf{M}^{-1}\mathbf{g}\left(\mathbf{x}^k\right) = \left(\mathbf{H}^T\mathbf{R}^{-1}\mathbf{H}\right)^{-1}\mathbf{H}^T\mathbf{R}^{-1}\left[\mathbf{z}-\mathbf{h}(\mathbf{x})\right] = \left[\mathbf{G}\left(\mathbf{x}^k\right)\right]^{-1}\mathbf{t}^k \quad (2.13)$$

$$\mathbf{G}\left(\mathbf{x}^k\right) = \mathbf{H}\left(\mathbf{x}^k\right)^T\mathbf{R}^{-1}\mathbf{H}\left(\mathbf{x}^k\right) \quad (2.14)$$

$$\mathbf{t}^k = \mathbf{H}^T\mathbf{R}^{-1}\left[\mathbf{z}^k-\mathbf{h}\left(\mathbf{x}^k\right)\right] \quad (2.15)$$

$$\mathbf{G}\left(\mathbf{x}^k\right)\Delta\mathbf{x}^k = \mathbf{t}^k \quad (2.16)$$

Where $\mathbf{G}(\mathbf{X}^k)$ is the Gain Matrix, $\Delta\mathbf{X}^k = \mathbf{X}^{k+1} - \mathbf{X}^k$ is the difference of the state estimate between iterations, and (2.16) is referred to as the Normal Equations. The iteration terminates when $\Delta\mathbf{x}k+1$ is below a pre-defined threshold.

The gain matrix can be used for observability analysis of the network, and it is crucial for static state estimation as its inversion is the most computational demanding part. According to [4], the gain matrix has the following properties:

- It is structurally and numerically symmetric.
- It is sparse, yet less sparse compared to **H**.
- In general it is a non-negative definite matrix, i.e. all of its eigenvalues are non-negative. It is positive definite for fully observable networks.

The sparsity of the gain matrix can be exploited to improve the computational efficiency and reduce the memory requirement. Details of the technique are given in [4].

2.1.4 The Measurement Jacobian Matrix

The measurement Jacobian matrix, **H**, as defined after (2.11) has the following structure:

$$\mathbf{z} = \begin{bmatrix} \frac{\partial \mathbf{P}_{inj}}{\partial \boldsymbol{\theta}} & \frac{\partial \mathbf{P}_{inj}}{\partial \mathbf{V}} \\ \frac{\partial \mathbf{Q}_{inj}}{\partial \boldsymbol{\theta}} & \frac{\partial \mathbf{Q}_{inj}}{\partial \mathbf{V}} \\ \frac{\partial \mathbf{P}_{flow}}{\partial \boldsymbol{\theta}} & \frac{\partial \mathbf{P}_{flow}}{\partial \mathbf{V}} \\ \frac{\partial \mathbf{Q}_{flow}}{\partial \boldsymbol{\theta}} & \frac{\partial \mathbf{Q}_{flow}}{\partial \mathbf{V}} \\ \mathbf{0} & \frac{\partial \mathbf{V}_{mag}}{\partial \mathbf{V}} \end{bmatrix} \qquad (2.17)$$

Based on the transmission line model shown in Figure 2-3, the expressions for each partition are given below:

1. Jacobian elements of the real power injection measurements:

$$\frac{\partial P_i}{\partial \theta_i} = -V_i \sum_{j=1}^{N} V_j (G_{ij} \sin\theta_{ij} - B_{ij} \cos\theta_{ij}) - V_i^2 B_{ii} \qquad (2.18)$$

$$\frac{\partial P_i}{\partial \theta_j} = V_i V_j (G_{ij} \sin\theta_{ij} - B_{ij} \cos\theta_{ij}) \qquad (2.19)$$

$$\frac{\partial P_i}{\partial V_i} = \sum_{j=1}^{N} V_j (G_{ij} \cos\theta_{ij} + B_{ij} \sin\theta_{ij}) + V_i G_{ii} \qquad (2.20)$$

$$\frac{\partial P_i}{\partial V_j} = V_i (G_{ij} \cos\theta_{ij} + B_{ij} \sin\theta_{ij}) \qquad (2.21)$$

2. Jacobian elements of the reactive power injection measurements:

$$\frac{\partial Q_i}{\partial \theta_i} = V_i \sum_{j=1}^{N} V_j (G_{ij} \cos\theta_{ij} + B_{ij} \sin\theta_{ij}) - V_i^2 G_{ii} \quad (2.22)$$

$$\frac{\partial Q_i}{\partial \theta_j} = -V_i V_j (G_{ij} \cos\theta_{ij} + B_{ij} \sin\theta_{ij}) \quad (2.23)$$

$$\frac{\partial Q_i}{\partial V_i} = \sum_{j=1}^{N} V_j (G_{ij} \sin\theta_{ij} - B_{ij} \cos\theta_{ij}) - V_i B_{ii} \quad (2.24)$$

$$\frac{\partial Q_i}{\partial V_j} = V_i (G_{ij} \sin\theta_{ij} - B_{ij} \cos\theta_{ij}) \quad (2.25)$$

3. Jacobian elements of the active power flow measurements:

$$\frac{\partial P_{ij}}{\partial \theta_i} = -\frac{V_i V_j}{a_{ij}} (-g_{ij} \sin\theta_{ij} + b_{ij} \cos\theta_{ij}) \quad (2.26)$$

$$\frac{\partial P_{ij}}{\partial \theta_j} = -\frac{V_i V_j}{a_{ij}} (g_{ij} \sin\theta_{ij} - b_{ij} \cos\theta_{ij}) \quad (2.27)$$

$$\frac{\partial P_{ij}}{\partial V_i} = 2\frac{V_i}{a_{ij}^2}(g_{si} + g_{ij}) - \frac{V_j}{a_{ij}} (g_{ij} \cos\theta_{ij} + b_{ij} \sin\theta_{ij}) \quad (2.28)$$

$$\frac{\partial P_{ij}}{\partial V_j} = -\frac{V_i}{a_{ij}} (g_{ij} \cos\theta_{ij} + b_{ij} \sin\theta_{ij}) \quad (2.29)$$

4. Jacobian elements of the reactive power flow measurements:

$$\frac{\partial Q_{ij}}{\partial \theta_i} = -\frac{V_i V_j}{a_{ij}} (g_{ij} \cos\theta_{ij} + b_{ij} \sin\theta_{ij}) \quad (2.30)$$

$$\frac{\partial Q_{ij}}{\partial \theta_j} = \frac{V_i V_j}{a_{ij}} (g_{ij} \cos\theta_{ij} + b_{ij} \sin\theta_{ij}) \quad (2.31)$$

$$\frac{\partial Q_{ij}}{\partial V_i} = -2\frac{V_i}{a_{ij}^2}(b_{si} + b_{ij}) - \frac{V_j}{a_{ij}} (g_{ij} \sin\theta_{ij} - b_{ij} \cos\theta_{ij}) \quad (2.32)$$

$$\frac{\partial Q_{ij}}{\partial V_j} = -\frac{V_i}{a_{ij}} (g_{ij} \sin\theta_{ij} - b_{ij} \cos\theta_{ij}) \quad (2.33)$$

5. Jacobian elements of the voltage magnitude measurements:

$$\frac{\partial V_i}{\partial V_i} = 1 \qquad (2.34)$$

$$\frac{\partial V_i}{\partial \theta_i} = \frac{\partial V_i}{\partial \theta_j} = \frac{\partial V_i}{\partial V_j} = 0 \qquad (2.35)$$

2.1.5 The WLS State Estimation Algorithm

Based on the network model and the mathematical models given in the previous sub-sections, the algorithm for WLS state estimation is outlined as follows [4]:

1. Start iterations, set the iteration index k = 0.
2. Initialize the state vector $\mathbf{X^k}$ typically as a flat start (all voltage angles equal to 0, and all voltage magnitudes equal to 1).
3. Formulate the Jacobian matrix, **H**, according to (2.17) to (2.35).
4. Calculate the gain matrix, $\mathbf{G}(\mathbf{X^k})$, using (2.14).
5. Calculate the estimated measurements based on $\mathbf{X^k}$,, $\mathbf{h}(\mathbf{X^k},)$, according to (2.1) to (2.9).
6. Calculate the right hand side $\mathbf{t^k}$using (2.15).
7. Decompose $\mathbf{G}(\mathbf{X^k})$ and solve for $\Delta \mathbf{X^k}$using (2.13).
8. Test for convergence, max $(|\Delta \mathbf{X^k}|) \leq \varepsilon$?
9. If Step 8 is not satisfied, update $\mathbf{X^{k+1}} = \mathbf{X^k} + \Delta \mathbf{X^k}$,k = k + 1, and go to Step 3. Else stop and output the state estimate.

2.2 Observability Analysis

Prior to state estimation, it must be guaranteed that a unique solution can be found with measurements received. The observability analysis is established for this purpose. The observability of the network can be defined on two levels. The first level is topological observability. A network is said to be topologically observable as long as enough measurements are placed at the right locations for a given network topology. The second level is numerical observability. The numerical observabilityrequires the gain matrix as defined in (2.14) to be non-singular, i.e. invertible. This not only requires the network to be topologically observable, but also free of outliers and gross measurement errors. As such cases are not likely to happen and could be easily prevented by checking the robustness of the state estimator and bad data analysis, only the topological observability is required and thus analysed for state estimation. In the following parts of the thesis, observability or network observability refers to topological observability for the sake of convenience.

In the case where the measurements available are not enough to support observability of the system, the network is divided into several Observable Islands separated by unobserved branches. Each of the observable islands has its individual reference angle, and the state estimation might still be performed within the observable islands. The observability analysis is also responsible for identifying the observable islands and finding measurements to restore the network observability.

As detailed in the Introduction, (topological) observability analysis can be carried out directly with the topological method that is based on the graphical theory, or using the numerical method based on the decoupled DC state estimation model and the measurement Jacobian matrix / the gain matrix.

The numerical observability analysis was first proposed in [26], where the theory behind observability analysis was presented, and the decoupled DC state estimation model was proposed for observability analysis. The observable islands and the unobserved branches are identified by partitioning the gain matrix and testing the observability of the sub-networks iteratively. The authors of [26] later improved the matrix partitioning process by using triangular factorisation [33]. Several methods based on the gain matrix have been proposed in [32], [34]-[35]. The other methods, which use alternative methods instead of analysing the gain matrix [36]-[37], include Hachtel's augmented matrix method [38]-[40], the gram matrix method and binary arithmetic [41].

It is reported in [42] that the classical method for observability analysis as proposed in [33] might incorrectly integrate the buses that belong to different observable islands into the same observable island. The cases in which the particular network topology and measurement placement would lead to misidentification of the observable islands are termed as pathological cases. It is stated in [42] that the pathological cases can be avoided by using the inverse triangular factors of the gain matrix instead of using the gain matrix directly, and the observable islands can be identified without iteration using the new method.

However, it is found that the method proposed in [42] still cannot prevent all pathological cases. In this section, a review of the classical method proposed in [33], and the improved method proposed in [42] is presented. A new method is proposed in this thesis, which is completely free of pathological cases and significantly faster than the existing methods, will be discussed in detail in Chapter 3.

2.2.1 Decoupled DC Model for Numerical Observability Analysis

The decoupled DC model was proposed in [96] as the simplified network model for observability analysis in state estimation. A linear relationship between the active power measurements and the states of voltage angle is assumed. As it is recognized that PV and Qθ are weakly coupled, while Pθ and QV are strongly coupled, only the equations related to active power measurements and voltage angle states are considered to further simplify the model. The decoupled DC model is helpful for numerical observability analysis because of its simplification in calculations without loss of topological information of the network. By neglecting the positions of the circuit breaker position, the observability of the network is not affected by the branch parameters and the values of the states. So, the decoupled DC model can be applied for simplifying observability analysis without introducing any error in terms of topological observability.

Using the decoupled DC model, the measurement equation as defined in (2.2) can be simplified as follows:

$$\mathbf{Z} = \mathbf{H}\boldsymbol{\theta} + \mathbf{e} \tag{2.36}$$

Where **Z** is the measurement vector containing the power injection and flow measurements only, **H** denotes the DC measurement Jacobian, **θ** is the state vector of voltage angles, and **e** is the error vector.

As the value of the state estimate does not affect the network topology and measurement locations, and thus the network observability, the measurement error covariance matrix (**R**) as defined after (2.10) can be assumed to be an identity matrix and this process does not introduce any errors. The gain matrix can then be simplified as follows:

$$\mathbf{G} = \mathbf{H}^{\mathbf{T}}\mathbf{H} \tag{2.37}$$

With unity branch reactance, the derivative of the power flow measurement is 1 for element corresponding to the sending bus, -1 for the receiving bus, and 0 for the other buses. As the power injection is the sum of the power flows into that bus, the derivative of the power injection measurement is N for the incident bus, -1 for the other ends of connected branches, and 0 for the other buses, where N is the number of the connecting branches of the incident bus. Examples of a power flow measurement and a power injection measurement are shown in (2.38) and (2.39), respectively.

$$\mathbf{h} = \begin{bmatrix} 0 & 0 & 0 & 0 & 1 & -1 \end{bmatrix} \tag{2.38}$$

$$\mathbf{h} = \begin{bmatrix} -1 & \cdots & -1 & N & 0 & \cdots & 0 & -1 & 0 & \cdots & 0 \end{bmatrix} \tag{2.39}$$

2.2.2 Factorisation of the Gain Matrix

In numerical observability analysis, a network can be seen as a combination of N observable islands (N=1 for fully observable case, N>1 for not fully observable case), each of the islands having their own reference angle. Thus, the gain matrix is always singular, and is required to be factorised in order to find information about the reference angles. In the classical method and the direct method presented in this section, Cholesky factorisation is used since the gain matrix is symmetrical. However, the prerequisite for Cholesky factorisation is that the matrix to be factorised must be positive definite. This problem is countered by skipping the zero pivot, and adding 0 into the corresponding diagonal element of the resulting diagonal matrix. For example, consider the case when the first zero pivot is encountered during factorisation as shown in (2.40).

$$\mathbf{D}_i = \mathbf{L}_1^{-1} \cdots \mathbf{L}_i^{-1} \mathbf{G} \mathbf{L}_i^{-T} \cdots \mathbf{L}_1^{-T} = \begin{bmatrix} d_1 & & & & \\ & \ddots & & & \\ & & d_i & & \\ & & & 0 & \mathbf{0} \\ & & & \mathbf{0} & \mathbf{G}_{i+1} \end{bmatrix} \tag{2.40}$$

Where **D** is the semi-factorised diagonal matrix whose first i elements have been factorised, d_i is the i^{th} diagonal element, $\mathbf{G}_i$ is the sub-matrix to be factorised in the i^{th} step, and $\mathbf{L}i$ is the Cholesky factor during the i^{th} step, whose structure is given in (2.41):

$$\mathbf{L}_i = \begin{bmatrix} \mathbf{I} & & \\ & 1 & \\ & \mathbf{l}_i & \mathbf{I} \end{bmatrix} \tag{2.41}$$

$$\mathbf{l}_i^T = \begin{bmatrix} L_{i+1,i} & \cdots & L_{N,i} \end{bmatrix} \tag{2.42}$$

Where N is the number of buses in the system, **I** denotes identity matrix of arbitrary size, $\mathbf{l}_i$ is a nonzero sub-vector under the element of 1 in the i^{th} column (size of (N-i-1)*1).

In this case, the factorisation process is continued by setting the i+1th element of the diagonal matrix to be zero and i^{th} Cholesky factor to be an identity matrix (2.43)-(2.44). In such a way, the factorisation at the i^{th} step is skipped, and the process may continue to factorise $\mathbf{G}i+1$.

$$d_{i+1} = 0 \tag{2.43}$$

$$\mathbf{L}_{i+1} = \mathbf{I} \tag{2.44}$$

Using this method for every zero pivot encountered, the resulting diagonal matrix can be expressed as follows:

$$\mathbf{D} = \mathbf{L}_1^{-1} \cdots \mathbf{L}_N^{-1} \mathbf{G} \mathbf{L}_N^{-T} \cdots \mathbf{L}_1^{-T} = \mathbf{L}^{-1} \mathbf{G} \mathbf{L}^{-T} \tag{2.45}$$

Where **D** is the resulting singular diagonal matrix, and **L** is the resulting lower triangular Cholesky factor. For analysis purposes, the zero pivots can be moved to the bottom of the **D** after proper matrix permutations (2.46); correspondingly the structure of **L** is given by (2.47):

$$\mathbf{D} = \begin{bmatrix} d_1 & & & \\ & \ddots & & \\ & & d_{N-k} & \\ & & & \mathbf{0}_k \end{bmatrix} \tag{2.46}$$

$$\mathbf{L} = \begin{bmatrix} 1 & & & \\ & \ddots & & \\ & & 1 & \\ \mathbf{l}_1 & \cdots & \mathbf{l}_{N-k} & \mathbf{I}_k \end{bmatrix} \tag{2.47}$$

Both **D** and **L** contain observability information of the network. How these matrices are used to identify the unobservable branches and the observable islands by the classical method and the direct method for observability analysis are described in detail in the following subsections. Details of each step of Cholesky factorisation are given in Appendix A.

2.2.3 The Classical Numerical Method for Observability Analysis

The classical numerical method for observability analysis is based on analysing the gain matrix. The network is observable if all branches are identified to be observable, or the observable islands are identified after the unobservable branches have been removed. The derivation of the classical model is given as follows [4]:

Consider the normal equation (2.16) expressed in the decouple DC model with all power flows set at 0:

$$\mathbf{G\theta} = \mathbf{t} = \mathbf{0} \tag{2.48}$$

As the angle of the reference bus is also included in the state vector, the gain matrix, **G**, is still singular even for the fully observable case. Thus, it is possible to partition the gain matrix after permuting the rows and columns properly:

$$\begin{bmatrix} \mathbf{G}_{11} & \mathbf{G}_{12} \\ \mathbf{G}_{21} & \mathbf{G}_{22} \end{bmatrix} \begin{bmatrix} \boldsymbol{\theta}_1 \\ \boldsymbol{\theta}_2 \end{bmatrix} = \begin{bmatrix} \mathbf{0} \\ \mathbf{0} \end{bmatrix} \tag{2.49}$$

$$\mathbf{G}_{22} \equiv \mathbf{0} \tag{2.50}$$

Where **G**11 is the maximum size non-singular sub matrix within **G**. The sub state vector, $\boldsymbol{\theta}_2$, is free to change its values as it is proved in [33] that its corresponding sub matrix of the gain matrix is always a zero matrix (2.50). Thus the value of $\boldsymbol{\theta}_1$ can also be determined by assigning arbitrary but different values to $\boldsymbol{\theta}_2$ as $\overline{\theta 2}$

$$\hat{\boldsymbol{\theta}}_1 = -\mathbf{G}_{11}^{-1}\mathbf{G}_{12}\bar{\boldsymbol{\theta}}_2 \tag{2.51}$$

Then the power flows of all branches with the solution can be calculated:

$$\mathbf{A}\begin{bmatrix} \hat{\boldsymbol{\theta}}_1^T & \bar{\boldsymbol{\theta}}_2^T \end{bmatrix}^T = \mathbf{A}\hat{\boldsymbol{\theta}}^* = \mathbf{P}_{branch} \tag{2.52}$$

Where **A** is the branch to bus incident matrix. Since it is assumed that all power flows in the network are equal to 0, the corresponding branches of the zero elements in **P** branch are identified as the unobservable branches.

As it is difficult to find **G**11, $\hat{\theta}^*$ can be solved using an alternative method, i.e. Cholesky factorisation of the gain matrix, **G**. The zero pivots in the resulting singular diagonal matrix, **D**, are replaced with 1's so that the gain matrix becomes invertible, and the corresponding elements of **t** are assigned with arbitrary but distinct values. The estimate of the state can be found using (2.53), and the values of $\bar{t}$are typically set as 0 for elements corresponding to positive pivots, and natural numbers starting from 1, as is shown in (2.54):

$$\hat{\boldsymbol{\theta}}^{*} = \left(\mathbf{L}\mathbf{D}\mathbf{L}^{T}\right)^{-1}\bar{\mathbf{t}} \tag{2.53}$$

$$\bar{\mathbf{t}}^{T} = \begin{bmatrix} 0 & \cdots & 0 & 1 & \cdots & N_{zp} \end{bmatrix} \tag{2.54}$$

Where N_{zp} is the number of zero pivots.

The unobservable branches identified that follow the above procedure might not include all unobservable branches. This is because the identification might be affected by the irrelevant injection measurements, the injection measurements incident to the unobservable branches. Thus, it is necessary to repeatedly identify the unobservable branches, eliminating the irrelevant injection measurements at the end of each time, until no more irrelevant injection measurements are identified.

Based on the methods introduced in this sub-section, the algorithm for classical numerical observability analysis is presented as follows:

1. Set the iteration number k = 1.
2. Form the gain matrix in decoupled DC model using (2.48).
3. Perform Cholesky factorisation on the gain matrix, substitute the zero pivots with 1, and assign natural numbers to the vector, **t**. If k = 1 and only one zero pivot is identified, stop the program, the network is fully observable. Else if k = 1 and more than one zero pivot is identified, go to Step 4, the network is not fully observable.
4. Identify the unobservable branches using (2.52) and (2.53), and the irrelevant injection measurements separated by the unobservable branches.
5. If no more unobservable branches are identified, then identify the observable islands separated by the unobservable branches. Else, k = k +1, go to Step 2.

2.2.4 The Direct Numerical Method for Observability Analysis

As suggested in [42], the classical method for observability analysis may incorrectly identify buses that belong to different observable islands in the same observable island. Consider a network with its gain matrix expressed by (2.55), the estimated angles can be derived as given in (2.56).

$$\mathbf{G} = \mathbf{L}\bar{\mathbf{D}}\mathbf{L}^{T} = \begin{bmatrix} 1 & & & \\ & \ddots & & \\ & & 1 & \\ \mathbf{l}_1 & \cdots & \mathbf{l}_{N-k} & \mathbf{I}_k \end{bmatrix} \begin{bmatrix} d_1 & & & \\ & \ddots & & \\ & & d_{N-k} & \\ & & & \mathbf{I}_k \end{bmatrix} \begin{bmatrix} 1 & & & \mathbf{l}_1^{T} \\ & \ddots & & \vdots \\ & & 1 & \mathbf{l}_{N-k}^{T} \\ & & & \mathbf{I}_k \end{bmatrix} \tag{2.55}$$

$$
\begin{aligned}
\hat{\boldsymbol{\theta}}^{*} &= \left(\mathbf{L}\bar{\mathbf{D}}\mathbf{L}^{T}\right)^{-1}\bar{\mathbf{t}} \\
&= \begin{bmatrix} 1 & & \mathbf{m}_1^T \\ & \ddots & \vdots \\ & 1 & \mathbf{m}_{N-k}^T \\ & & \mathbf{I}_k \end{bmatrix} \begin{bmatrix} d_1^{-1} & & \\ & \ddots & \\ & & d_{N-k}^{-1} \\ & & \mathbf{I}_k \end{bmatrix} \begin{bmatrix} 1 & & & \\ & \ddots & & \\ & & 1 & \\ \mathbf{m}_1 & \cdots & \mathbf{m}_{N-k} & \mathbf{I}_k \end{bmatrix} \begin{bmatrix} 0 \\ \vdots \\ 0 \\ \mathbf{n}_k \end{bmatrix} \\
&= \begin{bmatrix} 1 & & \mathbf{m}_1^T \\ & \ddots & \vdots \\ & 1 & \mathbf{m}_{N-k}^T \\ & & \mathbf{I}_k \end{bmatrix} \begin{bmatrix} 0 \\ \vdots \\ 0 \\ \mathbf{n}_k \end{bmatrix} \\
&= \begin{bmatrix} 1 & & \mathbf{u}_1^T & \mathbf{w}_1^T \\ & \ddots & \vdots & \vdots \\ & \ddots & \mathbf{u}_{N-k+1}^T & \mathbf{w}_{N-k+1}^T \\ & & 1 & \mathbf{w}_{N-k}^T \\ & & & \mathbf{I}_k \end{bmatrix} \begin{bmatrix} 0 \\ \vdots \\ \vdots \\ 0 \\ \mathbf{n}_k \end{bmatrix} \\
&= \begin{bmatrix} \mathbf{w}_1^T\mathbf{n}_k \\ \vdots \\ \mathbf{w}_{N-k}^T\mathbf{n}_k \\ \mathbf{n}_k \end{bmatrix}
\end{aligned}
\tag{2.56}
$$

where m_i is the sub-vector under the diagonal element of the i^{th} column of the matrix, ,L^{-1}, $\mathbf{w}_i$ is the sub-vector of m_i corresponding to the zero pivots, and $u_i$is the sub-vector of w_i that consists of the remaining elements, and $n_k$is a vector of natural numbers as given by (2.57).

$$\mathbf{n}_k^T = \begin{bmatrix} 1 & 2 & \cdots & k \end{bmatrix} \tag{2.57}$$

It can be seen from (2.56) that, although the values of the $\mathbf{w}_i$'s can be different, the results of the product might be the same. As will be proved in the next chapter, one of the properties of the $\mathbf{w}_i$ is that its sum of elements is always 1. Thus, it can be easily proved that for k> 2, such pathological cases might happen as multiple solutions can be found for $\mathbf{w}_i$ because its elements are only constrained by two equations.

$$\sum_{k=1}^{N} k w_{i,k} = C \tag{2.58}$$

$$\sum_{k=1}^{N} w_{i,k} = 1 \tag{2.59}$$

Where C is any real constant.

The above derivation also reveals that the sub-vectors, $\mathbf{w}_i$'s, might be the very key factors that contain information about observable islands. In [42], these sub-vectors and the bottom identity matrix are grouped together as the Test Matrix (2.60), and it is defined as the sub-matrix of the inverse of the Cholesky factor corresponding to the zero pivots. Note that, generally, the zero pivots might appear at any place on the diagonal matrix, **D**, and the columns of $\mathbf{I}_k$ might appear in any column in the test matrix.

$$\mathbf{W} = \begin{bmatrix} \mathbf{w}_1 & \mathbf{w}_2 & \cdots & \mathbf{w}_{N-k} & \mathbf{I}_k \end{bmatrix} \tag{2.60}$$

According to [42], the test matrix has the following two properties:

Property 1: The columns of **W** corresponding to buses that belong to the same observable island will have the same numerical values.

Property 2: The columns of **W** corresponding to buses that belong to different observable islands will have different numerical values, as long as these buses are connected by a common branch. If the buses are topologically separated, then their corresponding column vectors might be the same even though they belong to different observable islands.

Property 2 suggests that the observable islands might not be correctly identified even by directly comparing the column vectors of the test matrix. However, the identification of the unobservable branches can be directly identified using (2.61): the branches corresponding to non-zero row vectors are unobservable branches.

$$\mathbf{C} = \mathbf{A}\mathbf{W}^T \tag{2.61}$$

Where **A** is the branch to bus incident matrix.

Based on the two properties as proved in [42], the algorithm for the direct numerical observability analysis is presented as follows:

1. Form the gain matrix in decoupled DC model using (2.48).
2. Perform Cholesky factorisation on the gain matrix. If there is only one zero pivot, stop the program, the network is fully observable. Else, calculate the inverse matrix of the Cholesky factor and obtain the test matrix, **W**.
3. Calculate **C** using (2.61), find the non-zero row vectors of **C**, their corresponding branches are unobservable branches.
4. Identify the observable island separated by the unobservable branches.

2.2.5 Measurement Replacement

After the observable islands are identified, additional measurements should be replaced in order to restore the observability of the network. The candidate measurements include the power injection measurements incident to the border buses of the observable islands, and the power flow measurements that connect two observable islands. These candidate measurements can be expressed in a single matrix, $\mathbf{H}_c$.

Now consider the new gain matrix after all candidate measurements have been added into the network as expressed in (2.62).

$$\begin{aligned}\mathbf{G}_{new} &= \mathbf{G} + \mathbf{H}_c^T\mathbf{H}_c \\ &= \mathbf{L}\left(\mathbf{D} + \mathbf{L}^{-1}\mathbf{H}_c^T\left(\mathbf{L}^{-1}\mathbf{H}_c^T\right)^T\right)\mathbf{L}^T \\ &= \mathbf{L}\left(\begin{bmatrix}\bar{\mathbf{D}} & \\ & \mathbf{0}\end{bmatrix} + \begin{bmatrix}\mathbf{U}\mathbf{H}_c^T \\ \mathbf{W}\mathbf{H}_c^T\end{bmatrix}\begin{bmatrix}\mathbf{U}\mathbf{H}_c^T \\ \mathbf{W}\mathbf{H}_c^T\end{bmatrix}^T\right)\mathbf{L}^T \\ &= \mathbf{L}\begin{bmatrix}\bar{\mathbf{D}} + \mathbf{U}\mathbf{H}_c^T\mathbf{H}_c\mathbf{U}^T & \mathbf{U}\mathbf{H}_c^T\mathbf{H}_c\mathbf{W}^T \\ \mathbf{W}\mathbf{H}_c^T\mathbf{H}_c\mathbf{U}^T & \mathbf{W}\mathbf{H}_c^T\mathbf{H}_c\mathbf{W}^T\end{bmatrix}\mathbf{L}^T \\ &= \mathbf{L}\mathbf{E}\mathbf{L}^T\end{aligned} \tag{2.62}$$

where $\bar{\mathbf{D}}$ is the maximum non-singular submatrix of the singular diagonal matrix, **D**, **L** is the Cholesky factor, **W** is the test matrix, and **U** is the remaining part of $\mathbf{L}^{-1}$except for the test matrix.

1. Subtract $\mathbf{U}\mathbf{W}^{-1}$ times the second row from the first row:

$$\mathbf{E} = \begin{bmatrix}\bar{\mathbf{D}} + \mathbf{U}\mathbf{H}_c^T\mathbf{H}_c\mathbf{U}^T & \mathbf{U}\mathbf{H}_c^T\mathbf{H}_c\mathbf{W}^T \\ \mathbf{W}\mathbf{H}_c^T\mathbf{H}_c\mathbf{U}^T & \mathbf{W}\mathbf{H}_c^T\mathbf{H}_c\mathbf{W}^T\end{bmatrix} \sim \begin{bmatrix}\bar{\mathbf{D}} & \mathbf{0} \\ \mathbf{W}\mathbf{H}_c^T\mathbf{H}_c\mathbf{U}^T & \mathbf{W}\mathbf{H}_c^T\mathbf{H}_c\mathbf{W}^T\end{bmatrix} \tag{2.63}$$

2. Subtract $\bar{\mathbf{D}}^{-1}\mathbf{W}\mathbf{H}_c^T\mathbf{H}_c\mathbf{U}^T$ times the first row from the second row

$$\mathbf{E} \sim \begin{bmatrix}\bar{\mathbf{D}} & \mathbf{0} \\ \mathbf{W}\mathbf{H}_c^T\mathbf{H}_c\mathbf{U}^T & \mathbf{W}\mathbf{H}_c^T\end{bmatrix} \sim \begin{bmatrix}\bar{\mathbf{D}} & \mathbf{0} \\ \mathbf{0} & \left(\mathbf{H}_c\mathbf{W}^T\right)^T\mathbf{H}_c\mathbf{W}^T\end{bmatrix} \tag{2.64}$$

As $\bar{\mathbf{D}}$ and **L** are positive definite and rank(**A**) = rank($\mathbf{A}^T\mathbf{A}$), the new gain matrix will be observable, or it is 1 rank less than its dimension, as long as the matrix **B** as defined in (2.65) is observable. Since it is always more than enough to include all candidate measurements to restore network observability, only parts of them are required to be replaced. The selection of the necessary measurements can be done by computing the reduced echelon form $\mathbf{B}_e$ of **B**. The measurements corresponding to the linearly independent rows of $\mathbf{B}_e$ are the necessary measurements to be replaced.

$$\mathbf{B} = \mathbf{H}_c\mathbf{W}^T \tag{2.65}$$

Assuming the identification of observable islands have been done before the measurement replacement process, the algorithm for measurement replacement can be summarised as follows:

1. Find a list of candidate measurements, including the power flow and injection measurements incident to the observable islands that have been identified in the previous steps of observability analysis.
2. Form the candidate measurement Jacobian matrix, **H**c.
3. Assuming the test matrix **W** has already been calculated while identifying the observable islands, calculate **B** using (2.65), and its reduced echelon, **B**e. The measurements corresponding to the linearly independent rows of $\mathbf{B}_e$ are the minimum number of measurements that can restore the network observability.

2.2.6 Redundancy analysis.

After observability analysis a unique solution can be guaranteed with the measurements available. However, it is possible that some of the measurements might be lost due to telecommunication errors or failure of the measurement device. If a state is observed by only one measurement, then the loss of this measurement would make the system unobservable. In redundancy analysis, these measurements are termed as critical measurements, and the other type of measurements are termed as redundant measurements which can be removed without affecting the observability of the network [98].

Measurement redundancy is important for state estimation because it not only improves the reliability of state estimation, but also allows one of the essential functions of bad data detection. As will be discussed in detail in the next section, bad data detection uses measurement residuals to evaluate the magnitude of measurement errors. However, the residual of the critical measurement is always 0, making it impossible to detect any error in the critical measurements even if in the presence of large errors.

The redundant measurements can also be classified into different redundancy levels, including critical pairs, critical trios, and critical k-tuples, k = 4, 5, 6 … They are respectively defined as a set of two, three, and k measurements whose simultaneous removal from the measurement set would make the system unobservable. After the critical measurements are eliminated, the measurement redundancy level of the network could be enhanced by reducing the number of critical pairs, critical trios and critical k-tuples.

Assuming the network is fully observable after observability analysis, the reduced measurement Jacobian matrix, $\mathbf{H}_r$, with the column corresponding to the reference angle removed can be decomposed as expressed in (2.66) [98].

$$\mathbf{H}_d = \mathbf{L}^{-1}\mathbf{H}_r = \begin{bmatrix} \mathbf{I}_{N-1} \\ \mathbf{K}_{red} \end{bmatrix} \tag{2.66}$$

Where $\mathbf{I}_{N-1}$ is the identity matrix of size N-1, and $\mathbf{K}_{red}$ is the matrix of redundant measurements [99].

After the decomposition, the columns of $\mathbf{H}_d$ still correspond to the buses, and the rows of $\mathbf{H}_d$ still correspond to the measurements. The measurements corresponding to the identity matrix $\mathbf{I}_{N-1}$ are the selected set of basic of measurements that can make the system fully observable. If the elements of a column of $\mathbf{K}_{red}$ are all zeros, the corresponding state is a critical state, and the only measurement observing it, as indicated in the identity matrix, is a critical measurement. If a column of $\mathbf{K}_{red}$ contains k-1 nonzero elements, then the corresponding state of this column is a redundant state, and the basic measurement and the associated k-1 measurement form a critical k-tuple.

Extra measurements can be placed to eliminate the critical measurements and improve the measurement redundancy level. Similar to measurement replacement for network observability, the first step of redundancy improvement is to find a list of candidate measurements and form a reduced measurement Jacobian matrix $\mathbf{H}_{cr}$

excluding the reference angle. $\mathbf{H}_{cr}$ is combined to the bottom of $\mathbf{H}_{r}$, and the same triangular decomposition is performed for the augmented matrix as shown in (2.67):

$$\mathbf{H}_{ad} = \mathbf{L}^{-1}\begin{bmatrix}\mathbf{H}_{r}\\ \mathbf{H}_{cr}\end{bmatrix} = \begin{bmatrix}\mathbf{I}_{N-1}\\ \mathbf{K}_{red}\\ \mathbf{K}_{c}\end{bmatrix} \tag{2.67}$$

Where $\mathbf{H}_{ad}$ is the decomposed augmented measurement Jacobian matrix, and $\mathbf{K}_{c}$ is the matrix of candidate redundant measurements .

From $\mathbf{I}_{N-1}$, $\mathbf{K}_{red}$ and $\mathbf{K}_{c}$, a critical state to candidate measurement incident matrix **R** can be formed. The optimal placement of the measurements that eliminates the critical measurements can be found using integer linear programming (ILP) as stated below:

$$\begin{aligned}&\text{minimize } \mathbf{c}^{T}\mathbf{X}\\ &\text{subject to } \mathbf{RX} \geq \mathbf{1}\end{aligned} \tag{2.68}$$

Where **C** is a vector of costs for installing the measurements, **1** denotes a vector whose elements are all equal to 1, **X** is the vector consisting of binary decision variables xi that is defined as:

$$x_{i} = \begin{cases}1 \text{ if Measurement } i \text{ is included}\\ 0 \text{ if Measurement } i \text{ is not included}\end{cases} \tag{2.69}$$

Similar methods can be developed for improving the measurement redundancy to higher levels so as to eliminate the critical pairs, critical trios and so on by forming different incident matrices according to the redundancy level required.

2.3 Bad Data Detection and Identification

Measurements used in state estimation are constantly exposed to errors caused by different reasons, including the finite accuracy capability of the meters and the telecommunication medium. One of the most important functions of state estimation is to detect, identify and eliminate these errors. It is expected that a state estimator can filter out large errors, or bad data, as long as sufficient measurement redundancy is guaranteed.

The detection of the presence of data can be carried out using the statistical method of chi-squared distribution test, which will be discussed in Section 2.3.1. The following step of identification of the data that contains large errors using the normalised residual method is described further in Section 2.3.2.

Gross measurement errors can also be caused by meter wrong connections, telecommunication system failure, or topology and line parameter errors. Such errors are more complex, and must be handled by means of

topology estimation. Details of topology estimation will not be given in this work; readers can find them in [4], [100].

2.3.1 Bad Data Detection Using Chi-squared Distribution

Consider a vector **x** consisting of M random independent variables, in which every element xi follows the standard normal distribution [4], [101]:

$$x_i \sim N(0,1) \tag{2.70}$$

Then, a new random variable y following the chi-squared distribution of N degrees of freedom can be defined as:

$$y = \sum_{i=1}^{N} x_i^2 \sim \chi_N^2 \tag{2.71}$$

The degree of freedom M is decided by the number of independent random variables. Thus, if these variables are constrained by N independent equations, the degree of freedom would be reduced to M-N.

To illustrate the characteristics of chi-squared distribution, the chi-squared probability density function (p.d.f.) with 10 degrees of freedom is shown in Figure 2-4. The area under the p.d.f. is the probability of y having the value within the corresponding range. Since the tail of the curve is decaying, a threshold y_t can be set so that there is only a slight chance that the value of y will be greater than y_t. For example, in Figure 2-4 the threshold that divides the curve into the 95% region and 5% region is found at 18.3 for chi-squared distribution with 10 degrees of freedom. If the value of y is greater than this threshold, it is suspected that bad data exists in **x**.

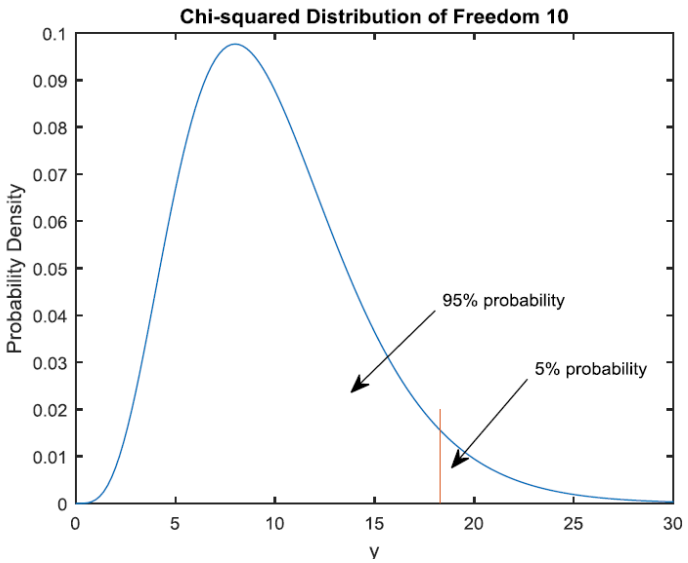

Figure 2-4: Chi-Squared Probability Density Function

Based on the assumption that measurement errors follow a Gaussian distribution, it can be found that the objective function as defined in (2.10) follows the chi-squared distribution with the degree of M-N:

$$J(\mathbf{x}) = [\mathbf{z} - \mathbf{h}(\mathbf{x})]^T \cdot \mathbf{R}^{-1} \cdot [\mathbf{z} - \mathbf{h}(\mathbf{x})]$$
$$= \mathbf{r}^T \mathbf{R}^{-1} \mathbf{r}$$
$$= \sum_{i=1}^{M} \left(\frac{r_i}{\sqrt{R_{ii}}} \right)^2 \quad (2.72)$$

$$\mathbf{r} = \mathbf{z} - \mathbf{h}(\mathbf{x}) \quad (2.73)$$

Where M is the number of measurements, N is the number of states, **r** is defined as the residual vector consisting of r_i's, i= 1, 2, … M, and the covariance matrix **R** is assumed to be diagonal and R_{ii} is its i^{th}diagonal element.

The degree of freedom of J(**x**) is M-N because the measurement equations must follow the N power balance equations. Thus, a threshold can be set according to the degree of freedom and the confidence level. The confidence level is usually set to be 95%, or it can be set to any number as required. The measurements are determined to be free of errors if J(**x**) is smaller than the threshold, or the existence of at least one set of bad data is detected.

2.3.2 Bad Data Identification with Largest Normalised Residual Test

The direct use of the objective function for chi-squared test might be inaccurate since the measurement error covariance matrix, **R**, is used to approximate the covariance of the measurement residuals, **Ω**. Consider the line arised measurement equation as given in (2.74). Using the WLS method, the estimate of Δ**x** can be expressed as given in (2.75), and the estimate of Δ**z** can be calculated as given in (2.76). The measurement residual can then be expressed as given in (2.77), and the exact expression of **Ω** is derived as given in (2.78).

$$\Delta \mathbf{z} = \mathbf{H}\Delta \mathbf{x} + \mathbf{e} \quad (2.74)$$

$$\Delta \hat{\mathbf{x}} = \left(\mathbf{H}^T \mathbf{R}^{-1} \mathbf{H} \right)^{-1} \mathbf{H}^T \mathbf{R}^{-1} \Delta \mathbf{z} \quad (2.75)$$

$$\Delta \hat{\mathbf{z}} = \mathbf{H}\Delta \hat{\mathbf{x}} = \mathbf{H}\left(\mathbf{H}^T \mathbf{R}^{-1} \mathbf{H} \right)^{-1} \mathbf{H}^T \mathbf{R}^{-1} \quad (2.76)$$

$$\mathbf{r} = \Delta \mathbf{z} - \Delta \hat{\mathbf{z}} = (\mathbf{I} - \mathbf{K})\Delta \mathbf{z}$$
$$= (\mathbf{I} - \mathbf{K})(\mathbf{H}\Delta \mathbf{x} + \mathbf{e})$$
$$= (\mathbf{I} - \mathbf{K})\mathbf{e} + \left[\mathbf{H}\left(\mathbf{H}^T \mathbf{R}^{-1} \mathbf{H} \right)^{-1} \mathbf{H}^T \mathbf{R}^{-1} \mathbf{H} + \mathbf{H} \right] \Delta \mathbf{x} \quad (2.77)$$
$$= (\mathbf{I} - \mathbf{K})\mathbf{e}$$
$$= \mathbf{S}e$$

$$\mathbf{\Omega} = \mathrm{cov}(\mathbf{r}) = \mathbf{S}\mathbf{R}\mathbf{S}^T = \mathbf{S}\mathbf{R} \quad (2.78)$$

Where **I** is the identity matrix, **$\Delta\hat{\mathbf{x}}$ and $\Delta\hat{\mathbf{z}}$** denote the estimate of Δ**x** and Δ**z**, respectively, and the matrix **S=I-K** is defined as the Residual Sensitivity Matrix [4].

Given the expression of **Ω**, the normalised residuals are defined as follows:

$$r_i^N = \frac{|r_i|}{\sqrt{\Omega_{ii}}} = \frac{|r_i|}{\sqrt{S_{ii}R_{ii}}} \tag{2.79}$$

Where $\mathbf{\Omega_{ii}}$ is the diagonal element of **Ω** and $\mathbf{r_i^N}$ is the normalised residual of the i^{th}element, which follows the Standard Normal Distribution:

$$r_i^N \sim N(0,1) \tag{2.80}$$

One of the most important properties of the normalised residuals is that the largest normalised residual will always correspond to the bad data. Consider the case where a large error is introduced in Measurement i: $e_i \neq 0$, while the errors existing in all of the other measurements are negligible: $e_j=0$, $j \neq i$. It is shown in (2.81) that the normalised residual of the bad data, which is Measurement k in this case, is always the largest among the normalised residuals of all measurements [4].

$$\begin{aligned} r_j^N &= \frac{|r_j|}{\sqrt{S_{jj}R_{jj}}} = \frac{S_{ji}e_i}{\sqrt{S_{jj}R_{jj}}} = \frac{\Omega_{ji}e_i}{\sqrt{\Omega_{jj}}R_{ii}} \\ &\leq \frac{\sqrt{\Omega_{jj}}\sqrt{\Omega_{ii}}e_i}{\sqrt{\Omega_{jj}}R_{ii}} \qquad \text{since } \Omega_{ji}^2 \leq \Omega_{jj}\Omega_{ii} \\ &= \frac{\sqrt{\Omega_{ii}}e_i}{R_{ii}} = \frac{S_{ii}e_i}{\sqrt{\Omega_{ii}}} = r_i^N \end{aligned} \tag{2.81}$$

This property can be used to identify bad data for any other types of redundant measurements except for critical measurements and critical pairs [102]. This is because, for the critical measurements, the normalised residual will always be 0, while for the critical pairs, the corresponding columns of **Ω** will be linearly dependant. The linear dependency can be expressed as given in (2.82), and it can be straightforwardly derived that the inequality in (2.81) becomes strict equality.

$$\begin{aligned} &\frac{\Omega_{ij}}{\Omega_{jj}} = \frac{\Omega_{ii}}{\Omega_{ji}} \\ &\rightarrow \Omega_{ji}^2 = \Omega_{jj}\Omega_{ii} \end{aligned} \tag{2.82}$$

Based on the properties of the normalised residuals described above, the algorithm for bad data identification can be summarised in the following steps:

1. Calculate the measurement residuals using (2.73).

2. Calculate the normalised residuals using (2.79).
3. Find the largest normalised residual r^N_{max}
4. If r^N_{max}> C , then the corresponding measurement is identified as bad data, else stop the program, no bad data is detected, where C is the threshold usually set to 3.
5. Eliminate or replace the erroneous measurement identified, and go back to Step1.

2.4 Conclusion

This chapter has given an overview of the classical state estimator that is realised by the WLS method, observability analysis and bad data detection and identification. In the following chapters, the network model, power flow equations as well as the WLS method will also be applied for constructing hybrid state estimators and dynamic state estimators. Based on the existing methods described in this chapter, new methods for numerical observability analysis are developed, and a new scheme for bad data detection and identification for dynamic state estimation is established.

References:

[1] A. G. Phadke and J. S. Thorp, Synchronised Phasor Measurements and Their Applications: Springer, 2008.

[2] A. Monticelli, "Electric power system state estimation", Proc. IEEE, vol. 88, no. 2, pp. 262-282, 2000-Feb.

[3] Monticelli, A. (1999). State Estimation in Electric Power Systems, Springer US.

[4] A. Abur and A. Gomez-Exposito, Power System State Estimation: Theory and Implementation. New York: Marcel Dekker, 2004.

[5] A. Wood and B. F. Wollenberg, Power Generation Operation and Control, 2nd ed, 1996.

[6] F. C. Schweppe and J. Wildes, "Power System Static-State Estimation, Part I: Exact Model," in the IEEE Transactions on Power Apparatus and Systems, vol. PAS-89, no. 1, pp. 120-125, Jan. 1970.

[7] F. C. Schweppe and D. B. Rom, "Power System Static-State Estimation, Part II: Approximate Model," in the IEEE Transactions on Power Apparatus and Systems, vol. PAS-89, no. 1, pp. 125-130, Jan. 1970.

[8] F. C. Schweppe, "Power System Static-State Estimation, Part III: Implementation," in the IEEE Transactions on Power Apparatus and Systems, vol. PAS-89, no. 1, pp. 130-135, Jan. 1970.

[9] Y.-F. Huang, S. Werner, J. Huang, N. Kashyap, V. Gupta, "State estimation in electric power grids: Meeting new challenges presented by the requirements of the future grid" in the IEEE Signal Process. Mag., vol. 29, no. 5, pp. 33-43, 2012.

[10] A. Q. Huang, "Power Semiconductor Devices for Smart Grid and Renewable Energy Systems," in Proceedings of the IEEE, vol. 105, no. 11, pp. 2019-2047, Nov. 2017.

[11] E. Ghahremani and I. Kamwa, "Local and Wide-Area PMU-Based Decentralized Dynamic State Estimation in Multi-Machine Power Systems," in the IEEE Transactions on Power Systems, vol. 31, no. 1, pp. 547-562, Jan. 2016.

[12] M. Asprou, "Synchronised measurement technology: A blessing for power systems [Trends in Future I&M]," in the IEEE Instrumentation & Measurement Magazine, vol. 20, no. 3, pp. 25-42, June 2017.

[13] M. Asprou, S. Chakrabarti and E. Kyriakides, "A Two-Stage State Estimator for Dynamic Monitoring of Power Systems," in the IEEE Systems Journal, vol. 11, no. 3, pp. 1767-1776, Sept. 2017.

[14] F. F. Wu and W. H. E. Liu, "Detection of topology errors by state estimation power systems]," in the IEEE Transactions on Power Systems, vol. 4, no. 1, pp. 176-183, Feb 1989.

[15] R. E. Larson, W. F. Tinney and J. Peschon, "State Estimation in Power Systems Part I: Theory and Feasibility," in the IEEE Transactions on Power Apparatus and Systems, vol. PAS-89, no. 3, pp. 345-352, March 1970.

[16] R. E. Larson, W. F. Tinney, L. P. Hajdu and D. S. Piercy, "State Estimation in Power Systems Part II: Implementation and Applications," in the IEEE Transactions on Power Apparatus and Systems, vol. PAS-89, no. 3, pp. 353-363, March 1970.

[17] O. J. M. Smith, "Power System State Estimation," in the IEEE Transactions on Power Apparatus and Systems, vol. PAS-89, no. 3, pp. 363-379, March 1970.

[18] L. Zhang, A. Bose, A. Jampala, V. Madani and J. Giri, "Design, Testing, and Implementation of a Linear State Estimator in a Real Power System," in the IEEE Transactions on Smart Grid, vol. 8, no. 4, pp. 1782-1789, July 2017.

[19] T. Yang, H. Sun and A. Bose, "Transition to a Two-Level Linear State Estimator—Part I: Architecture," in the IEEE Transactions on Power Systems, vol. 26, no. 1, pp. 46-53, Feb. 2011.

[20] T. Yang, H. Sun and A. Bose, "Transition to a Two-Level Linear State Estimator—Part II: Algorithm," in the IEEE Transactions on Power Systems, vol. 26, no. 1, pp. 54-62, Feb. 2011.

[21] M. Zhou, V. A. Centeno, J. S. Thorp and A. G. Phadke, "An Alternative for Including Phasor Measurements in State Estimators," in the IEEE Transactions on Power Systems, vol. 21, no. 4, pp. 1930-1937, Nov. 2006.

[22] T.S. Bi, X.H. Qin, Q.X. Yang, A novel hybrid state estimator for including synchronised phasor measurements, Electric Power Systems Research, Volume 78, Issue 8, 2008, Pages 1343-1352, ISSN 0378-7796, http://dx.doi.org/10.1016/j.epsr.2007.12.002.

[23] M. Asprou and E. Kyriakides, "Enhancement of hybrid state estimation using pseudo flow measurements," 2011 IEEE Power and Energy Society General Meeting, San Diego, CA, 2011, pp. 1-7.

[24] S. Chakrabarti, E. Kyriakides, G. Ledwich and A. Ghosh, "Inclusion of PMU current phasor measurements in a power system state estimator," in IET Generation, Transmission & Distribution, vol. 4, no. 10, pp. 1104-1115, October 2010.

[25] G. Valverde, S. Chakrabarti, E. Kyriakides and V. Terzija, "A Constrained Formulation for Hybrid State Estimation," in the IEEE Transactions on Power Systems, vol. 26, no. 3, pp. 1102-1109, Aug. 2011.

[26] A. Monticelli and F. F. Wu, "Network Observability: Theory," Power Engineering Review, IEEE, vol. PER-5, pp. 32-33, 1985.

[27] G. R. Krumpholz, K. A. Clements, and P. W. Davis, "Power System Observability: A Practical Algorithm Using Network Topology," Power Apparatus and Systems, IEEE Transactions on, vol. PAS-99, pp. 1534-1542, 1980.

[28] A. M. Sasson, S. T. Ehrmann, P. Lynch, and L. S. Van Slyck, "Automatic Power System Network Topology Determination," Power Apparatus and Systems, IEEE Transactions on, vol. PAS-92, pp. 610-618, 1973.

[29] V. H. Quintana, A. Simoes-Costa, and A. Mandel, "Power System Topological Observability Using a Direct Graph-Theoretic Approach," Power Engineering Review, IEEE, vol. PER-2, pp. 23-23, 1982.

[30] K. A. Clements, G. R. Krumpholz, and P. W. Davis, "Power System State Estimation with Measurement Deficiency: An Algorithm that Determines the Maximal Observable Subnetwork," Power Apparatus and Systems, IEEE Transactions on, vol. PAS-101, pp. 3044-3052, 1982.

[31] K. A. Clements, G. R. Krumpholz, and P. W. Davis, "Power System State Estimation with Measurement Deficiency: An Observability/Measurement Placement Algorithm," Power Engineering Review, IEEE, vol. PER-3, pp. 28-28, 1983.

[32] I. W. Slutsker and J. M. Scudder, "Network Observability Analysis through Measurement Jacobian Matrix Reduction," IEEE Transactions on Power Systems, vol. 2, pp. 331-336, 1987.

[33] A. Monticelli and F. F. Wu, "Network Observability: Identification of Observable Islands and Measurement Placement," Power Engineering Review, IEEE, vol. PER-5, pp. 32-32, 1985.

[34] F. F. Wu, W. H. E. Liu, and S. M. Lun, "Observability analysis and bad data processing for state estimation with equality constraints," IEEE Transactions on Power Systems, vol. 3, pp. 541-548, 1988.

[35] D. M. Falcao and M. A. Arias, "State estimation and observability analysis based on echelon forms of the linearized measurement models," IEEE Transactions on Power Systems, vol. 9, pp. 979-987, 1994.

[36] F. F. Wu, W. H. E. Liu, L. Holten, L. Gjelsvik, and S. Aam, "Observability analysis and bad data processing for state estimation using Hachtel's augmented matrix method," IEEE Transactions on Power Systems, vol. 3, pp. 604-611, 1988.

[37] R. R. Nucera, V. Brandwajn, and M. L. Gilles, "Observability and bad data analysis using augmented blocked matrices [power system analysis computing]," IEEE Transactions on Power Systems, vol. 8, pp. 426-433, 1993.

[38] M. C. d. Almeida, E. N. Asada, and A. V. Garcia, "On the Use of Gram Matrix in Observability Analysis," IEEE Transactions on Power Systems, vol. 23, pp. 249-251, 2008.

[39] M. Almeida, E. Asada, and A. Garcia, "Power system observability analysis based on gram matrix and minimum norm solution," in Power & Energy Society General Meeting, 2009.PES '09. IEEE, 2009, pp. 1-1.

[40] G. N. Korres, "A Gram Matrix-Based Method for Observability Restoration," IEEE Transactions on Power Systems, vol. 26, pp. 2569-2571, 2011.

[41] C. Solares, A. J. Conejo, E. Castillo, and R. E. Pruneda, "Binary-arithmetic approach to observability checking in state estimation," IET Generation, Transmission & Distribution, vol. 3, pp. 336-345, 2009.

[42] B. Gou and A. Abur, "A Direct Numerical Method for Observability Analysis," IEEE TRANSACTIONS ON POWER SYSTEMS, VOL. 15, NO. 2, MAY 2000.

[43] V. Terzija et al., "Wide-Area Monitoring, Protection, and Control of Future Electric Power Networks," in Proceedings of the IEEE, vol. 99, no. 1, pp. 80-93, Jan. 2011.

[44] V. Terzija, Z. M. Radojević and G. Preston, "Flexible Synchronised Measurement Technology-Based Fault Locator," in the IEEE Transactions on Smart Grid, vol. 6, no. 2, pp. 866-873, March 2015.

[45] A. Moreno-Munoz, V. Pallares-Lopez, J. J. Gonzalez de la Rosa, R. Real-Calvo, M. Gonzalez-Redondo and I. M. Moreno-Garcia, "Embedding Synchronised Measurement Technology for Smart Grid Development," in the IEEE Transactions on Industrial Informatics, vol. 9, no. 1, pp. 52-61, Feb. 2013.

[46] S. Chakrabarti, E. Kyriakides, T. Bi, D. Cai and V. Terzija, "Measurements get together," in the IEEE Power and Energy Magazine, vol. 7, no. 1, pp. 41-49, January-February 2009.

[47] J. De La Ree, V. Centeno, J. S. Thorp and A. G. Phadke, "Synchronised Phasor Measurement Applications in Power Systems," in the IEEE Transactions on Smart Grid, vol. 1, no. 1, pp. 20-27, June 2010.

[48] J. S. Thorp, A. G. Phadke, S. H. Horowitz and M. M. Begovic, "Some applications of phasor measurements to adaptive protection," in the IEEE Transactions on Power Systems, vol. 3, no. 2, pp. 791-798, May 1988.

[49] W. Dickerson, "Effect of PMU analog input section performance on frequency and ROCOF estimation error," 2015 IEEE International Workshop on Applied Measurements for Power Systems (AMPS), Aachen, 2015, pp. 31-36.

[50] A. Sharma, S. C. Srivastava and S. Chakrabarti, "A multi-agent-based power system hybrid dynamic state estimator," in the IEEE Intelligent Systems, vol. 30, no. 3, pp. 52-59, May-June 2015.

[51] S. Naka, T. Genji, T. Yura and Y. Fukuyama, "A hybrid particle swarm optimisation for distribution state estimation," in the IEEE Transactions on Power Systems, vol. 18, no. 1, pp. 60-68, Feb 2003.

[52] C.-H. Lin, "A distributed state estimator for electric power systems" in the IEEE Trans. Power Syst., vol. 7, no. 2, pp. 551-557, May 1992.

[53] X. Li and A. Scaglione, "Robust Decentralized State Estimation and Tracking for Power Systems via Network Gossiping," in the IEEE Journal on Selected Areas in Communications, vol. 31, no. 7, pp. 1184-1194, July 2013.

[54] D. Falcao, F. Wu, L. Murphy, "Parallel and distributed state estimation" in the IEEE Trans. Power Syst., vol. 10, no. 2, pp. 724-730, May 1995.

[55] G. Korres, A. Tzavellas, E. Galinas, "A distributed implementation of multi-area power system state estimation on a cluster of computers", Elect. Power Syst. Res., vol. 102, pp. 20-32, Sep. 2013.

[56] W. Jiang, V. Vittal, G. Heydt, "A distributed state estimator utilizing synchronised phasor measurements" in the IEEE Trans. Power Syst., vol. 22, no. 2, pp. 563-571, May 2007.

[57] W. Jiang, V. Vittal, G. Heydt, "Diakoptic state estimation using phasor measurement units" in the IEEE Trans. Power Syst., vol. 23, no. 4, pp. 1580-1589, Nov. 2008.

[58] L. Xie, D.-H. Choi, S. Kar, H. V. Poor, "Fully distributed state estimation for wide-area monitoring systems" in the IEEE Trans. Smart Grid, vol. 3, no. 3, pp. 1154-1169, 2012.

[59] V. Basetti and A. K. Chandel, "Hybrid power system state estimation using Taguchi differential evolution algorithm," in IET Science, Measurement & Technology, vol. 9, no. 4, pp. 449-466, 7 2015.

[60] E. Ghahremani and I. Kamwa, "PMU analytics for decentralized dynamic state estimation of power systems using the Extended Kalman Filter with Unknown Inputs," 2015 IEEE Power & Energy Society General Meeting, Denver, CO, 2015, pp. 1-5.

[61] A. K. Singh and B. C. Pal, "Decentralized Dynamic State Estimation in Power Systems Using Unscented Transformation," in the IEEE Transactions on Power Systems, vol. 29, no. 2, pp. 794-804, March 2014

[62] E. Ghahremani and I. Kamwa, "Local and Wide-Area PMU-Based Decentralized Dynamic State Estimation in Multi-Machine Power Systems," in the IEEE Transactions on Power Systems, vol. 31, no. 1, pp. 547-562, Jan. 2016.

[63] Y. Chakhchoukh, V. Vittal and G. T. Heydt, "PMU Based State Estimation by Integrating Correlation," in the IEEE Transactions on Power Systems, vol. 29, no. 2, pp. 617-626, March 2014.

[64] E. Ghahremani and I. Kamwa, "PMU analytics for decentralized dynamic state estimation of power systems using the Extended Kalman Filter with Unknown Inputs," 2015 IEEE Power & Energy Society General Meeting, Denver, CO, 2015, pp. 1-5.

[65] J. Du, S. Ma, Y. C. Wu and H. V. Poor, "Distributed Hybrid Power State Estimation Under PMU Sampling Phase Errors," in the IEEE Transactions on Signal Processing, vol. 62, no. 16, pp. 4052-4063, Aug.15, 2014.

[66] V. Basetti and A. K. Chandel, "Hybrid power system state estimation using Taguchi differential evolution algorithm," in IET Science, Measurement & Technology, vol. 9, no. 4, pp. 449-466, 7 2015

[67] Wei Li, Luigi Vanfretti, A PMU-based state estimator considering classic HVDC links under different control modes, Sustainable Energy, Grids and Networks, Volume 2, June 2015, Pages 69-82, ISSN 2352-4677, http://dx.doi.org/10.1016/j.segan.2015.04.004.

[68] V. Donde, X. Feng, I. Segerqvist and M. Callavik, "Distributed State Estimation of Hybrid AC/HVDC Grids by Network Decomposition," in the IEEE Transactions on Smart Grid, vol. 7, no. 2, pp. 974-981, March 2016.

[69] S. J. Huang and K. R. Shih, "Dynamic-state-estimation scheme including nonlinear measurement-function considerations," in IEE Proceedings - Generation, Transmission and Distribution, vol. 149, no. 6, pp. 673-678, Nov 2002.

[70] P. Rousseaux, T. Van Cutsem, and T. E. DyLiacco, "Whither dynamic state estimation?," International Journal of Electrical Power & Energy Systems, vol. 12, no. 2, pp. 104-116, Apr. 1990.

[71] A. S. Debs and R. E. Larson, "A Dynamic Estimator for Tracking the State of a Power System," in the IEEE Transactions on Power Apparatus and Systems, vol. PAS-89, no. 7, pp. 1670-1678, Sept. 1970.

[72] W. Miller and J. Lewis, "Dynamic state estimation in power systems," in the IEEE Transactions on Automatic Control, vol. 16, no. 6, pp. 841-846, Dec 1971.

[73] M. F. Allam and M. A. Laughton, "Power-system dynamic-state estimation by optimal variable incremental displacements," in Electrical Engineers, Proceedings of the Institution of, vol. 123, no. 5, pp. 433-436, May 1976.

[74] M. F. Allam and M. A. Laughton, "Power-system dynamic-state estimation by optimal variable incremental displacements," in Electrical Engineers, Proceedings of the Institution of, vol. 123, no. 5, pp. 433-436, May 1976.

[75] K. Nishiya, J. Hasegawa and T. Koike, "Dynamic state estimation including anomaly detection and identification for power systems," in IEE Proceedings C - Generation, Transmission and Distribution, vol. 129, no. 5, pp. 192-198, September 1982.

[76] A. M. L. da Silva, M. B. D. C. Filho and J. M. C. Cantera, "An Efficient Dynamic State Estimation Algorithm Including Bad Data Processing," in the IEEE Power Engineering Review, vol. PER-7, no. 11, pp. 49-49, Nov. 1987.

[77] A. K. Sinha and J. K. Mondal, "Dynamic state estimator using ANN based bus load prediction," in the IEEE Transactions on Power Systems, vol. 14, no. 4, pp. 1219-1225, Nov 1999.

[78] F. Aminifar, M. Shahidehpour, M. Fotuhi-Firuzabad and S. Kamalinia, "Power System Dynamic State Estimation With Synchronised Phasor Measurements," in the IEEE Transactions on Instrumentation and Measurement, vol. 63, no. 2, pp. 352-363, Feb. 2014.

[79] L. Hu, Z. Wang and X. Liu, "Dynamic State Estimation of Power Systems With Quantization Effects: A Recursive Filter Approach," in the IEEE Transactions on Neural Networks and Learning Systems, vol. 27, no. 8, pp. 1604-1614, Aug. 2016.

[80] R. Huang, G. Cokkinides, C. Hedrington and S. A. P. Meliopoulos, "Distribution System Distributed Quasi-Dynamic State Estimator," in the IEEE Transactions on Smart Grid, vol. 7, no. 6, pp. 2761-2770, Nov. 2016.

[81] J. Zhao, M. Netto and L. Mili, "A Robust Iterated Extended Kalman Filter for Power System Dynamic State Estimation," in the IEEE Transactions on Power Systems, vol. 32, no. 4, pp. 3205-3216, July 2017.

[82] E. Ghahremani and I. Kamwa, "Local and Wide-Area PMU-Based Decentralized Dynamic State Estimation in Multi-Machine Power Systems," in the IEEE Transactions on Power Systems, vol. 31, no. 1, pp. 547-562, Jan. 2016.

[83] M. A. M. Ariff, B. C. Pal and A. K. Singh, "Estimating Dynamic Model Parameters for Adaptive Protection and Control in Power System," in the IEEE Transactions on Power Systems, vol. 30, no. 2, pp. 829-839, March 2015.

[84] N. Zhou, D. Meng, Z. Huang and G. Welch, "Dynamic State Estimation of a Synchronous Machine Using PMU Data: A Comparative Study," in the IEEE Transactions on Smart Grid, vol. 6, no. 1, pp. 450-460, Jan. 2015.

[85] S. A. A. Shahriari, M. Raoofat, M. Dehghani, M. Mohammadi and M. Saad, "Dynamic state estimation of a permanent magnet synchronous generator-based wind turbine," in IET Renewable Power Generation, vol. 10, no. 9, pp. 1278-1286, 10 2016.

[86] Y. Cui, R. G. Kavasseri and S. M. Brahma, "Dynamic State Estimation Assisted Out-of-Step Detection for Generators Using Angular Difference," in the IEEE Transactions on Power Delivery, vol. 32, no. 3, pp. 1441-1449, June 2017.

[87] N. Zhou, D. Meng and S. Lu, "Estimation of the Dynamic States of Synchronous Machines Using an Extended Particle Filter," in the IEEE Transactions on Power Systems, vol. 28, no. 4, pp. 4152-4161, Nov. 2013.

[88] G. Anagnostou; B. C. Pal, "Derivative-free Kalman filtering based Approaches to Dynamic State Estimation for Power Systems with Unknown Inputs," in the IEEE Transactions on Power Systems , vol.PP, no.99, pp.1-1

[89] E. Ghahremani and I. Kamwa, "Dynamic State Estimation in Power System by Applying the Extended Kalman Filter With Unknown Inputs to Phasor Measurements," in the IEEE Transactions on Power Systems, vol. 26, no. 4, pp. 2556-2566, Nov. 2011.

[90] A. Rouhani and A. Abur, "Observability Analysis for Dynamic State Estimation of Synchronous Machines," in the IEEE Transactions on Power Systems, vol. 32, no. 4, pp. 3168-3175, July 2017.

[91] J. Qi, K. Sun and W. Kang, "Optimal PMU Placement for Power System Dynamic State Estimation by Using Empirical ObservabilityGramian," in the IEEE Transactions on Power Systems, vol. 30, no. 4, pp. 2041-2054, July 2015.

[92] H. Chen, M. Liu and S. Zhang, "Event-triggered distributed dynamic state estimation with imperfect measurements over a finite horizon," in IET Control Theory & Applications, vol. 11, no. 15, pp. 2607-2622, 10 13 2017.

[93] H. Modir and R. A. Schlueter, "A Dynamic State Estimator for Dynamic Security Assessment," in the IEEE Transactions on Power Apparatus and Systems, vol. PAS-100, no. 11, pp. 4644-4652, Nov. 1981.

[94] Wikipedia, Available: https://en.wikipedia.org/wiki/Stochastic_process.

[95] Wikipedia, Available: https://en.wikipedia.org/wiki/Random_variable.

[96] G. C. Contaxis and G. N. Korres, "A reduced model for power system observability: analysis and restoration," IEEE Transactions on Power Systems, vol. 3, pp. 1411-1417, 1988.

[97] A. Chakrabortty, P. Khargoneka, "Introduction to wide-area control of power systems", Proc. Amer. Control Conf., pp. 6773-6785, 2013.

[98] J. Chen and A. Abur, "Placement of PMUs to Enable Bad Data Detection in State Estimation," in the IEEE Transactions on Power Systems, vol. 21, no. 4, pp. 1608-1615, Nov. 2006.

[99] N. G. Bretas and J. B. A. London, "Measurement placement design and reinforcement for state estimation purposes," 2001 IEEE Porto Power Tech Proceedings (Cat. No.01EX502), Porto, 2001, pp. 6 pp. vol.3-.

[100] E. Handschin, F.C. Schweppe, J. Kohlas, and A. Fiechter, "Bad data analysis for power system state estimation," IEEE Transactions on Power Apparatus and Systems, vol. 94, no. 2, pp. 329-337, May 1975.

[101] A. Monticelli, State Estimation in Electric Power Systems: A Generalized Approach. Massachusetts: Kluwer Academic Publishers, 1999.

[102] K. A. Clements and P. W. Davis, "Multiple Bad Data Detectability and Identifiability, A Geometric Approach," in the IEEE Power Engineering Review, vol. PER-6, no. 7, pp. 73-73, July 1986.

[103] M.C. de Almeida, E.N. Asada, A.V. Garcia, On the use of Gram matrix in observability analysis, IEEE Trans. Power Syst. 23 (2008) 249–251.

[104] M.C. de Almeida, E.N. Asada, A.V. Garcia, Power system observability analysis based on Gram matrix and minimum norm solution, IEEE Trans. Power Syst. 23 (2008) 1611–1618.

[105] G. N. Korres. A Gram matrix-based method for observability restoration," IEEE Transactions on Power Systems, vol. 26, no. 4, pp. 2569-2571, Nov. 2011.

[106] G. C. Contaxis, G. N. Korres, A reduced model for power system observability analysis and restoration, IEEE Trans. Power Syst. 3 (1988) 1411–1417.

[107] E. Castillo, A.J. Conejo, R.E. Pruneda, C. Solares, State estimation observability based on the null space of the measurement Jacobian matrix, IEEE Trans. Power Syst. 20 (2005) 1656–1658.

[108] E. Castillo, A.J. Conejo, R.E. Pruneda, C. Solares, Observability analysis in state estimation: a unified numerical approach, IEEE Trans. Power Syst. 21 (2006) 877–886.

[109] G. N. Korres.An integer-arithmetic algorithm for observability analysis of systems with SCADA and PMU measurements. Electric Power Systems Research, Vol. 81, pp. 1388-1402, March 2011.

[110] B. Gou, "Jacobian matrix-based observability analysis for state estimation," in the IEEE Transactions on Power Systems, vol. 21, no. 1, pp. 348-356, Feb. 2006.

[111] G. Strang, Linear Algebra and Its Applications, 3rd Edition ed.: Harcourt Brace Jovanovich, 1988.

[112] Z.Jin; P.Dattaray; P.Wall; J.Yu; V.Terzija, "A Screening Rule Based Iterative Numerical Method for Observability Analysis," in the IEEE Transactions on Power Systems , vol.PP, no.99, pp.1-1.

[113] Pserc.cornell.edu.(2017). Index for Directory matpower5.0. [online] Available at: http://www.pserc.cornell.edu/matpower/docs/ref/matpower5.0/menu5.0.html [Accessed 22 Nov. 2015].

[114] Manousakis, N.M.; Korres, G.N.; Georgilakis, P.S., "Taxonomy of PMU Placement Methodologies," in Power Systems, IEEE Transactions on Power Systems, vol.27, no.2, pp.1070-1077, May 2012.

[115] R. Sodhi, S. C. Srivastava, and S. N. Singh, “Optimal PMU placement to ensure system observability under contingencies,” in Proc. IEEE Power Eng. Soc. General Meeting, 2009, pp. 1–6.

[116] F. Aminifar, A. Khodaei, M. Fotuhi-Firuzabad, and M. Shahidehpour, “Contingency-constrained PMU placement in power networks,” IEEE Trans. Power Syst., vol. 25, no. 1, pp. 516–523, Feb. 2010.

[117] D. Dua, S. Dambhare, R. K. Gajbhiye, and S. A. Soman, “Optimal multistage scheduling of PMU placement: An ILP approach,” IEEE Trans. Power Del., vol. 23, no. 4, pp. 1812–1820, Oct. 2008.

[118] R. Emami and A. Abur, “Robust measurement design by placing synchronised phasor measurements on network branches,” IEEE Trans. Power Syst., vol. 25, no. 1, pp. 38–43, Feb. 2010.

[119] S. Chakrabarti, D. Eliades, E. Kyriakides, and M. Albu, “Measurement uncertainty considerations in optimal sensor deployment for state estimation,” in Proc. IEEE Int. Symp.Intelligent Signal Processing, 2007.

[120] S. Chakrabarti, E. Kyriakides, and D. G. Eliades, “Placement of synchronised measurements for power system observability,” IEEE Trans. Power Del., vol. 24, no. 1, pp. 12–19, Jan. 2009.

[121] B. Milosevic and M. Begovic, "Nondominated sorting genetic algorithm for optimal phasor measurement placement," in the IEEE Transactions on Power Systems, vol. 18, no. 1, pp. 69-75, Feb 2003.

[122] Mahdi Hajian, Ali Mohammad Ranjbar, TurajAmraee, BabakMozafari, Optimal placement of PMUs to maintain network observability using a modified BPSO algorithm, In International Journal of Electrical Power & Energy Systems, Volume 33, Issue 1, 2011, Pages 28-34, ISSN 0142-0615, https://doi.org/10.1016/j.ijepes.2010.08.007.

[123] I. Kamwa and R. Grondin, "PMU configuration for system dynamic performance measurement in large, multiarea power systems," in the IEEE Transactions on Power Systems, vol. 17, no. 2, pp. 385-394, May 2002.

[124] R. F. Nuqui, A. G. Phadke, R. P. Schulz and N. Bhatt, "Fast on-line voltage security monitoring using synchronised phasor measurements and decision trees," 2001 IEEE Power Engineering Society Winter Meeting. Conference Proceedings (Cat.No.01CH37194), Columbus, OH, 2001, pp. 1347-1352 vol.3.

[125] C. Rakpenthai, S. Premrudeepreechacharn, S. Uatrongjit and N. R. Watson, "An Optimal PMU Placement Method Against Measurement Loss and Branch Outage," in the IEEE Transactions on Power Delivery, vol. 22, no. 1, pp. 101-107, Jan. 2007.

[126] N. H. Abbasy and H. M. Ismail, "A unified approach for the optimal PMU location for power system state estimation," IEEE Trans. Power Syst., vol. 24, no. 2, pp. 806–813, May 2009.

[127] G. B. Denegri, M. Invernizzi and F. Milano, "A security oriented approach to PMU positioning for advanced monitoring of a transmission grid," Proceedings. International Conference on Power System Technology, 2002, pp. 798-803 vol.2.

[128] M. Korkali and A. Abur, "Placement of PMUs with channel limits," in Proc. IEEE Power Eng. Soc. General Meeting, 2009.

[129] M. Korkali and A. Abur, "Impact of network sparsity on strategic placement of phasor measurement units with fixed channel capacity," in Proc. IEEE Int. Symp. Circuits and Syst. (ISCAS), 2010, pp. 3445–3448.

[130] K.-S. Cho, J.-R. Shin, and S. H. Hyun, "Optimal placement of phasor measurement units with GPS receiver," Proc. IEEE Power Eng. Soc. Winter Meeting, pp. 258–262, 2001.

[131] H.-S. Zhao, Y. Li, Z.-Q. Mi, and L. Yu, "Sensitivity constrained PMU placement for complete observability of power systems," in Proc. IEEE Power Eng. Soc. Transm.Distrib. Conf. Exhib., 2005.

[132] R. Kavasseri, S. K. Srinivasan, "Joint optimal placement of PMU and conventional measurements in power systems", Proc. IEEE Int. Symp.Circuits and Syst. (ISCAS), pp. 3449-3452, 2010.

[133] F. Aminifar, M. Fotuhi-Firuzabad, M. Shahidehpour, A. Khodaei, "Probabilistic multistage PMU placement in electric power systems", IEEE Trans. Power Del., vol. 26, no. 2, pp. 841-849, Apr. 2011.

[134] S. Chakrabarti, E. Kyriakides, "Optimal placement of phasor measurement units for power system observability", IEEE Trans. Power Syst., vol. 23, no. 3, pp. 1433-1440, Aug. 2008.

[135] J. Peng, Y. Sun, H. F. Wang, "Optimal PMU placement for full network observability using Tabu search algorithm", Int. J. Elect. Power Energy Syst., vol. 28, no. 4, pp. 223-231, May 2006.

[136] K.-S. Cho, J.-R. Shin, S. H. Hyun, "Optimal placement of phasor measurement units with GPS receiver", Proc. IEEE Power Eng. Soc. Winter Meeting, pp. 258-262, 2001.

[137] H.-S. Zhao, Y. Li, Z.-Q. Mi, L. Yu, "Sensitivity constrained PMU placement for complete observability of power systems", Proc. IEEE Power Eng. Soc. Transm.Distrib. Conf. Exhib., 2005.

[138] C. Peng, H. Sun, J. Guoa, "Multi-objective optimal PMU placement using a non-dominated sorting differential evolution algorithm", Int. J. Elect. Power Energy Syst., vol. 32, no. 8, pp. 886-892, Oct. 2010.

[139] M. Hajian, A. M. Ranjbar, T. Amraee, B. Mozafari, "Optimal placement of PMUs to maintain network observability using a modified BPSO algorithm", Int. J. Elect. Power Energy Syst., vol. 33, no. 1, pp. 28-34, Jan. 2011.

[140] A. Ahmadi, Y. Alinejad-Beromi, M. Moradi, "Optimal PMU placement for power system observability using binary particle swarm optimisation and considering measurement redundancy", Expert Syst. Appl., vol. 38, pp. 7263-7269, 2011.

[141] F. Aminifar, C. Lucas, A. Khodaei, M. Fotuhi-Firuzabad, "Optimal placement of phasor measurement units using immunity genetic algorithm", IEEE Trans. Power Del., vol. 24, no. 3, pp. 1014-1020, Jul. 2009.

[142] M. Zhou, V. A. Centeno, A. G. Phadke, Y. Hu, D. Novosel, H. A. R. Volskis, "A preprocessing method for effective PMU placement studies", Proc. IEEE Int. Conf. Electric Utility Deregulation Restructuring Power Technologies, pp. 2862-2867, 2008.

[143] B. Gou, "Generalized integer linear programming formulation for optimal PMU placement," IEEE Trans. Power Syst., vol. 23, no. 3, pp. 1099–1104, Aug. 2008.

[144] B. Gou, "Optimal placement of PMUs by integer linear programming," IEEE Trans. Power Syst., vol. 23, no. 3, pp. 1525–1526, Aug. 2008.

[145] B. Xu and A. Abur, "Observability analysis and measurement placement for systems with PMUs," IEEE PES Power Systems Conference and Exposition, 2004., 2004, pp. 943-946 vol.2.

[146] RanjanaSodhi, S.C. Srivastava, S.N. Singh, Optimal PMU placement method for complete topological and numerical observability of power system, In Electric Power Systems Research, Volume 80, Issue 9, 2010, Pages 1154-1159, ISSN 0378-7796, https://doi.org/10.1016/j.epsr.2010.03.005.

[147] J. Chen, A. Abur, "Improved bad data processing via strategic placement of PMUs", Proc. IEEE Power Eng. Soc. General Meeting, pp. 509-513, 2005.

[148] J. Chen, A. Abur, "Placement of PMUs to enable bad data detection in state estimation", IEEE Trans. Power Syst., vol. 21, no. 4, pp. 1608-1615, Nov. 2006.

[149] I. Kamwa, R. Grondin, "PMU configuration for system dynamic performance measurement in large multiarea power systems", IEEE Trans. Power Syst., vol. 17, no. 2, pp. 385-394, May 2002.

[150] W. Jiang, V. Vittal, G. T. Heydt, "A distributed state estimator utilizing synchronised phasor measurements", IEEE Trans. Power Syst., vol. 22, no. 2, pp. 1-6, May 2007.

[151] University of Washington.Power Systems Test Case Archive. Available: https://www.ee.washington.edu/research/pstca/, 2015

[152] A. G. Phadke, J. S. Thorp, R. F. Nuqui, and M. Zhou, "Recent developments in state estimation with phasor measurements," in Power Systems Conference and Exposition, 2009. PSCE '09. IEEE/PES, 2009, pp. 1-7.

[153] A. Gómez-Expósito, A. Abur, and P. Rousseaux, "On the use of PMUs in power system state estimation," presented at the Proc. Power Systems Computation Conf., Stockholm, Sweden, 2011.

[154] S. G. Ghiocel, J. H. Chow, G. Stefopoulos, B. Fardanesh, D. Maragal, B. Blanchard, M. Razanousky, and D. B. Bertagnolli, "Phasor-Measurement-Based State Estimation for Synchrophasor Data Quality Improvement and Power Transfer Interface Monitoring," Power Systems, IEEE Transactions on, vol. 29, pp. 881-888, 2014.

[155] L. Vanfretti, J. H. Chow, S. Sarawgi, and B. Fardanesh, "A Phasor-Data-Based State Estimator Incorporating Phase Bias Correction," Power Systems, IEEE Transactions on, vol. 26, pp. 111-119, 2011.

[156] S. Di, D. J. Tylavsky, and N. Logic, "An Adaptive Method for Detection and Correction of Errors in PMU Measurements," Smart Grid, IEEE Transactions on, vol. 3, pp. 1575-1583, 2012.

[157] Kirincic, V., Skok, S. &Frankovic, D. (2016). A Synchrophasor Assisted Hybrid State Estimator. Journal of Electrical Engineering, 67(2), pp. 103-110.

[158] A. Simões Costa, A. Albuquerque and D. Bez, "An estimation fusion method for including phasor measurements into power system real-time modeling," in the IEEE Transactions on Power Systems, vol. 28, no. 2, pp. 1910-1920, May 2013.

[159] J. Du, S. Ma, Y. C. Wu and H. V. Poor, "Distributed Hybrid Power State Estimation Under PMU Sampling Phase Errors," in the IEEE Transactions on Signal Processing, vol. 62, no. 16, pp. 4052-4063, Aug.15, 2014.

[160] A. G. Phadke and J. S. Thorp, Computer relaying for Power Systems: Research Sudies Press, Somerset, England, 1988.

[161] J. S. Thorp and A. G. Phadke, "Real-time voltage phasor measurements for static state estimation," IEEE Transactions on Power Apparatus and Systems, vol. Vol. 104, No. 11, November 1985, pp. 3098-3017, 1985.

[162] A. G. Phadke and J. S. Thorp, "State estimation with phasor measurements," IEEE Transactions on Power Apparatus and Systems, vol. Vol. 1, No.1, pp. 233-241, 1986.

[163] M. Göl and A. Abur, "Observability and Criticality Analyses for Power Systems Measured by Phasor Measurements," in the IEEE Transactions on Power Systems, vol. 28, no. 3, pp. 3319-3326, Aug. 2013.

[164] J. K. Mandal, A. K. Sinha and L. Roy, "Incorporating nonlinearities of measurement function in power system dynamic state estimation," in IEE Proceedings - Generation, Transmission and Distribution, vol. 142, no. 3, pp. 289-296, May 1995.

[165] G. Valverde and V. Terzija, "Unscented Kalman filter for power system dynamic state estimation," in IET Generation, Transmission & Distribution, vol. 5, no. 1, pp. 29-37, Jan. 2011.

[166] N.G. Bretas, An iterative dynamic state estimation and bad data processing, International Journal of Electrical Power & Energy Systems, Volume 11, Issue 1, 1989, Pages 70-74, ISSN 0142-0615, http://dx.doi.org/10.1016/0142-0615(89)90010-0.

[167] Gelb, A. (1974).Applied Optimal Estimation, MIT Press.

[168] P. Rousseaux, Th. Van Cutsem, T.E. DyLiacco, Whither dynamic state estimation?, International Journal of Electrical Power & Energy Systems, Volume 12, Issue 2, 1990.

[169] A. K. Singh and B. C. Pal, "Decentralized dynamic state estimation in power systems using unscented transformation," 2014 IEEE PES General Meeting | Conference & Exposition, National Harbor, MD, 2014, pp. 1-1.

[170] A. Mam, B. Pal and A. Singh, "Estimating dynamic model parameters for adaptive protection and control in power system," 2015 IEEE Power & Energy Society General Meeting, Denver, CO, 2015, pp. 1-1.

[171] A. M. Leite da Silva, M. B. Do CouttoFilho, and J. F. de Queiroz, "State forecasting in electric power systems," IEE Proceedings on Generation, Transmission and Distribution, vol. 130, no. 5, pp. 237-244, Sept. 1983.

[172] I. Arasaratnam and S. Haykin, "Cubature Kalman Filters," in